A Robust Hybrid Machine and Deep Learning-based Model for Classification and Identification of Chest X-ray Images

Rana Jassim Mohammed
Department of Computer Science, College of Education for Pure Sciences, University of Basrah, Basrah, 61004, Iraq
rana.mohammed@uobasrah.edu.iq

Mudhafar Jalil Jassim Ghrabat
Iraqi Commission for Computers and Informatics, The Informatics Institute for Postgraduate Studies, Baghdad 10013, Iraq | Computer Science Department, Al-Turath University, Baghdad 10013, Iraq
mudhafar.jalil@iips.icci.edu.iq

Zaid Ameen Abduljabbar
Department of Computer Science, College of Education for Pure Sciences, University of Basrah, Basrah, 61004, Iraq
zaid.ameen@uobasrah.edu.iq

Vincent Omollo Nyangaresi
Department of Computer Science and Software Engineering, Jaramogi Oginga Odinga University of Science & Technology, Bondo 40601, Kenya | Department of Applied Electronics, Saveetha School of Engineering, SIMATS, Chennai, Tami lnadu 602105, India
vnyangaresi@jooust.ac.ke

Iman Qays Abduljaleel
Department of Computer Science, College of Education for Pure Sciences, University of Basrah, Basrah, 61004, Iraq
iman.abduljaleel@uobasrah.edu.iq

Ali Hasan Ali
Department of Mathematics, College of Education for Pure Sciences, University of Basrah, Basrah, 61004, Iraq | Institute of Mathematics, University of Debrecen, Pf. 400, H-4002 Debrecen, Hungary
ali.hasan@science.unideb.hu

Dhafer G. Honi
Department of Computer Science, College of Education for Pure Sciences, University of Basrah, Basrah, 61004, Iraq | Department of IT, University of Debrecen, Debrecen, 4002, Hungary
dhafer.honi@uobasrah.edu.iq

Husam A. Neamah
Department of Electrical Engineering and Mechatronics, Faculty of Engineering, University of Debrecen, Debrecen, 4028, Otemeto u.4-5, Hungary
husam@eng.unideb.hu (corresponding author)

Received: 13 May 2024 | Revised: 17 June 2024 | Accepted: 20 June 2024

 DOI: https://doi.org/10.48084/etasr.7828

ABSTRACT

Successful medical treatment for patients with COVID-19 requires rapid and accurate diagnosis. Fighting the COVID-19 pandemic requires an automated system to diagnose the virus on Chest X-Ray (CXR) images. CXR images are frequently used in healthcare as they offer the potential for rapid and accurate disease diagnosis. SARS-CoV-2 targets the respiratory system, resulting in pneumonia with additional symptoms, such as dry cough, fatigue, and fever, which could be misdiagnosed as pneumonia, TB, or lung cancer. There is difficulty in differentiating the features of COVID-19 from other diseases that have similarities in CXR images. Automated Computer-Aided Diagnosis (CAD) systems incorporate machine or deep learning methods to improve efficiency and accuracy. CNNs are among the most widely used methods, as they have shown encouraging accuracy in identifying COVID-19 in CXR images. This study presents a hybrid deep learning model to provide faster diagnosis of COVID-19 infection using CXR images. The Densenet201 model was used for feature extraction and a Multi-Layer Perceptron (MLP) was used for classification. The proposed method achieved 98.82% accuracy and similar sensitivity, specificity, precision, recall, and F1 score. These results are promising when compared to other DL models trained in similar datasets.

Keywords-COVID-19; Chest X-Ray (CXR); DL; ML; densenet201; MLP

I. INTRODUCTION

More than 670 million illnesses and no less than 6.8 million deaths have been attributed to COVID-19 [1]. Polymerase Chain Reaction (PCR) is the present gold standard for detecting and diagnosing SARS-CoV-2 [2]. However, PCR tests can produce false negative results [3]. Obtaining correct clinical results with high efficiency is very important. The large number of patients infected with COVID-19 requires the correct use of resources and the provision of quality services to maintain the safety of both infected patients and health workers. Lung tomography is of indisputable diagnostic significance in the identification of many diseases [4]. The benefits of AI-based methods include lower cost, availability, and ease of use in a variety of therapeutic settings, including both community and hospital settings. The implementation of such approaches in a high-volume diagnostic environment could be self-limiting because, although any doctor can get a clinical impression from XR images, the results must be validated by a radiologist. The speed of results validation is based on the availability of radiologists and the size of the images to be examined [5-10]. Due to this, the automatic identification of lung disorders using AI is an extremely significant concept that is regularly explored in the disciplines of medical informatics and radiology [11]. The COVID-19 epidemic can be better managed with a prompt and accurate diagnosis using CXR images and symptoms, helping healthcare systems protect vulnerable people. AI can be used in many different ways to analyze complicated data and learn more about COVID-19. AI utilizes Machine Learning (ML) and Deep Learning (DL) to develop algorithms that can be applied in the biomedical and clinical domains to classify and stratify patients using a variety of data sources. Using AI to identify high-risk patients early, treat them, and control the spread of the disease is an important contribution. Furthermore, AI can help with pandemic management by promptly alerting authorities of COVID-19 outbreaks [12-13]. CXR images are used to classify patients with COVID-19, and the results show that ML and DL algorithms perform very well and accurately.

A. Research Motivation

In the context of image classification, the availability of extensive and well-labeled datasets enables the selection of more relevant features, resulting in better differentiation between image categories. This leads to the formation of more distinct groups of results, enhancing the accuracy of predictions for new and unseen images. The limited and uneven availability of datasets in medical data results in generalization errors. However, models trained on diversified datasets are capable of learning in a general manner, and the boundaries between classes are also distinct. As a result, ML and DL models can use the characteristics and classification skills of pre-trained models while dealing with excessively large datasets.

B. Research Contribution

This study proposes a hybrid model using DenseNet and MLP to detect COVID-19 in CXR data. The first phase of the DL-based diagnosis of MERS-CoV (COVID-19) is detection, followed by classification in connection to chest disorders, including normal, pneumonia, and COVID-19. This study is an improved version of [14]. This study:

- Combines the pre-trained DenseNet201 CNN model for feature extraction and the MLP model for classification.
- Achieves a high level of accuracy (98.82%) when applied to the NIH dataset.

II. LITERATURE REVIEW

In [15], CoviNet was introduced, which is a deep learning network capable of detecting COVID-19 in CXR images. This architecture was based on CNN, histogram equalization, and an adaptive median filter. In terms of binary classification, the model was 98.62% accurate, while in terms of multiclass classification, it was 95.77% accurate. In [16], traditional ML models were combined with pre-trained DL to automatically diagnose COVID-19 from CXR images. The features retrieved were chosen and classified to improve decision-making for infectious diseases, such as bacterial and viral pneumonia. A fresh CXR database was built to test this method, which achieved a success rate of more than 99%. In [17], the EfficientNet architecture was used to detect COVID-19 in chest CT images, achieving 0.897 accuracy, 0.896 F1 score, and 0.895 AUC. Using the reduce-on-plateau learning rate optimization method, which involves slowing down learning when model performance stops improving, the F1 score was

0.9, while it was 0.8 and 0.82 when using the cyclic learning rate and constant learning rate, respectively. In [18], a Gaussian filter was used to reduce image noise and improve quality. In [19], a CNN was combined with popular ML techniques such as Bayes, RF, KNN, and MLP. The InceptionV3 architecture with an SVM classifier using a linear kernel achieved 99.42% accuracy, making it the best extractor-classifier combo, while ResNet50 with MLP achieved 97.46% accuracy. In [20], DL and transfer learning were combined to diagnose COVID-19 on CXR images. The VGG16 architecture was modified, achieving 99.7% accuracy. In [21], the Xception, InceptionV3, and MobileNetv3 models achieved 91%, 89%, and 86% accuracy, respectively. In [22], a thorough training approach was followed to achieve a multiclass classification of respiratory diseases. Cutting and resizing procedures were employed in the initial preprocessing stage to remove any extraneous information from the samples. A pre-trained EfficientNet v2 network was used to generate a nominal feature set and assign the correct categories to subsequent images. The three categories were classified more accurately using this technique. However, the algorithm had performance and customization limitations that worsened as class sizes increased. Deep learning techniques can improve the quality and utility of fused images. In [23], a modified AlexNet architecture was used for feature extraction and classification in a dataset with four classes. According to [24], smartphone apps based on ML models can help diagnose COVID-19, diabetes, and heart diseases. In [25], a novel end-to-end CNN model was used to classify CXR images, obtaining 97% sensitivity and 99.32% specificity, which shows promise compared to other DL models on the same dataset. In [26], the CXR-EffDet model was proposed to identify and classify eight different types of chest deformity using X-rays. EfficientDet-D0, based on EfficientNet-B0, was used to calculate a specific set of key point samples and complete the classification task. Furthermore, this method was adaptable in identifying a range of CXR abnormalities, as it used a single-stage object identifier to detect different chest diseases. However, its performance was lower in images with hazy effects. In general, deep learning models greatly enhance the accuracy and pace of COVID-19 diagnosis from medical images, achieving accuracy rates of more than 95%. Such models can be essential to identify infected people and isolate them to prevent the virus from spreading. However, further research must improve the robustness and generalizability of models [27]. Many AI frameworks have been successfully used to detect COVID-19 in CXR CT images with remarkable precision. However, there are still obstacles that must be overcome, such as the inability of algorithms to process larger classes, the requirement for real-time predictions, and the criticality of validating results in real-world healthcare environments. Although these developments enhance the efficacy and dependability of diagnostics, ongoing research is needed to tackle these obstacles and further optimize these methods. Models must generalize to diverse populations to be applicable globally, an aspect that is often missing and poorly addressed in existing models. Despite the advances made, the gap between deployments to real-life healthcare processes is huge. The interpretability of AI models is a critical specification to ensure that healthcare professionals can rely on and understand AI predictions. Patient data privacy is a major concern when publishing CXR images to train a model [28]. Covid forecasting involves some markers, such as epidemiological data (incidence and prevalence data), genomic surveillance, vaccination coverage, and the impact of public health policies, such as social distancing, mask mandates, and travel restrictions. In addition, certain trends related to travel, migration, weather, and seasonality may play an important role in the transmission of infectious diseases. Furthermore, access to healthcare and public health infrastructure is affected by socioeconomic factors. Combining these characteristics into models would allow researchers to better predict the timing and impact of a pandemic so that they can better prepare and respond [29-30].

III. METHOD

This study investigates the classification of CXR images, which is a crucial task in identifying cases of normality, pneumonia, and COVID-19. The DenseNet201 and Multi-Layer Perceptron (MLP) were used to improve classification accuracy. During the preprocessing steps, SMOTE was used to balance data effectively and the images were downsized to a standard 128×128×3 resolution. Classified cross-entropy loss and accuracy in training and validation were used to evaluate the model, along with the F1 score, sensitivity, specificity, loss, accuracy, and precision. Figure 1 shows the entire process followed. The proposed model is called NIH CXR.

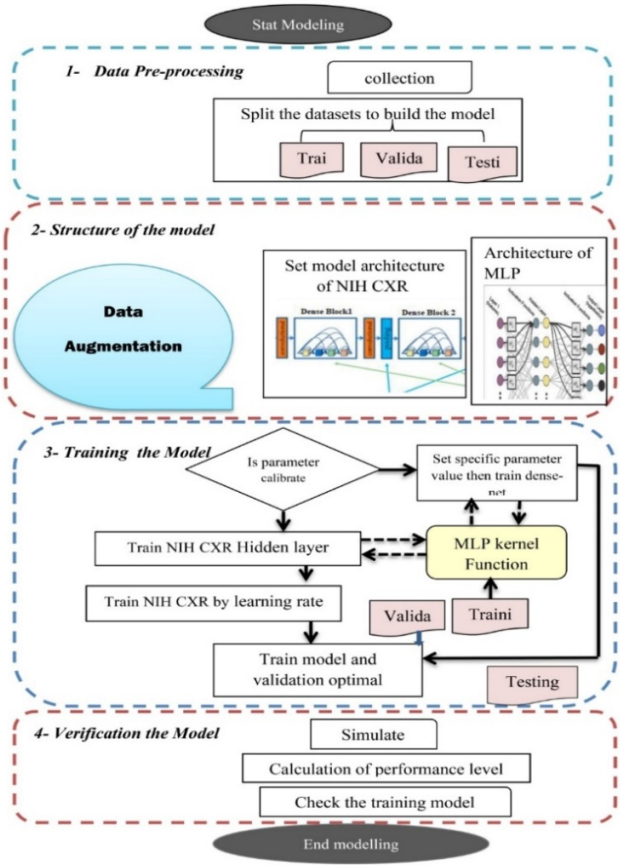

Fig. 1. Flowchart of the proposed method for COVID-19 detection on CXR images.

A. Data Collection

The NIH CXR dataset includes 112,120 radiographs from 30,805 distinct patients who had received pathologic diagnoses for experimental purposes. To generate these designations, natural language processing was used on the texts of disease classifications from relevant radiological reports. After preprocessing, the data was divided into separate sets for training, validation, and testing purposes. Table II shows the categories in the dataset, while Figure 2 shows sample images from the categories.

TABLE I. DATASET CATEGORIES

Category	Count
Normal	6000
COVID-19	5634
Pneumonia	5000

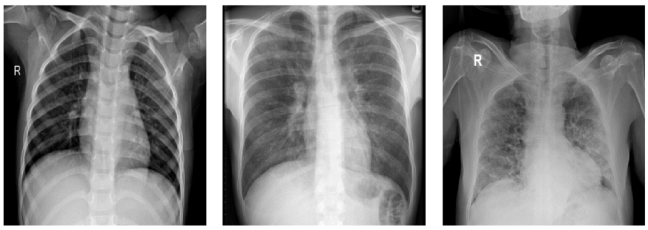

(a) (b) (c)

Fig. 2. Sample images of the dataset: (a) Normal image, (b) pneumonia image, (c) COVID-19 image.

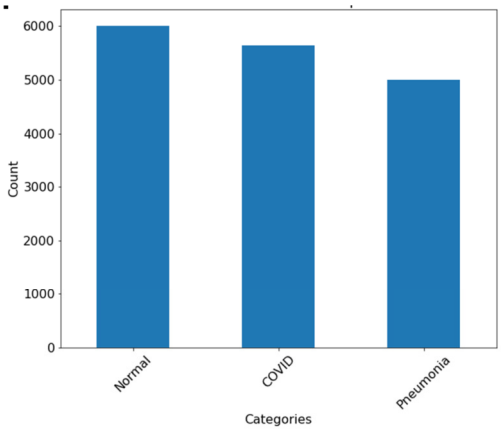

Fig. 3. Data distribution before data sampling.

B. Data Preprocessing

Preprocessing was performed to enhance the performance of the proposed system. Images were resized, horizontally and vertically flipped, and rotated 25°. All images were scaled to 128×128×3 using the Pyldic library to match the framework requirements. After normalizing each pixel of each image to the interval, the images were all transformed into an array data format [0, 1]. Typically, the underrepresented class receives a low classification. The SMOTE oversampling technique was used to balance the dataset. SMOTE was proposed to generate minority-specific synthetic examples according to feature affinity in minority-specific values [25]. Figure 5 shows the data per category after applying SMOTE. Addressing class imbalance and high dimensionality of data are standardization tools to improve diagnostic performance and scalability [31].

C. Data Split

The dataset was divided into training (60%), validation (20%), and testing (20%) subsets. The training set (60%) was used to teach the ML model by letting it pick up relationships, patterns, and features. The validation set (20%) was used to test the model after training to adjust hyperparameters, avoid overfitting, and gauge generalization to new data. The test set (20%) was reserved for use only after training and validation, to evaluate the model's final performance on unseen data.

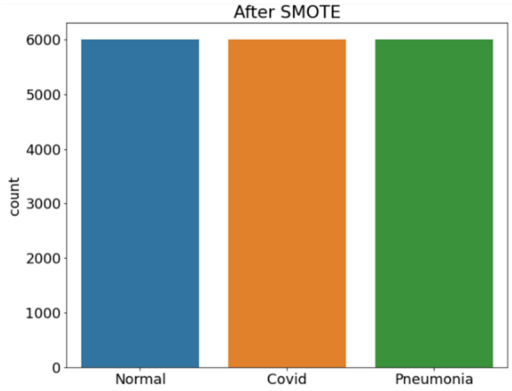

Fig. 4. Data balancing after using SMOTE sampling.

D. Design of the Model

The selection of the number of layers in a neural network architecture to detect COVID-19 in CXR images varies in different aspects. Layers can be stacked according to the task complexity and the volume of the dataset [32]. In complicated tasks with more data, deeper networks could capture more detailed patterns. Cross-validation is used to ensure that the architecture generalizes to new data Regularization methods, such as dropout and batch normalization, can be used to reduce overfitting and stiffness in deeper networks. Experiments can even be used to change the number of layers according to performance improvement and computation cost [33].

1) DenseNet201

The DenseNet architecture is characterized by dense connectivity patterns between layers. DenseNet201 is made up of numerous dense blocks, with interconnected sets of convolutional layers inside each dense block. A transition layer takes the output from every dense block and uses a convolutional layer and a pooling operation to lower the feature maps' spatial dimensions. The last dense block is succeeded by a global average pooling layer that, after averaging the feature maps across all spatial dimensions, yields a one-dimensional vector. This vector is then inputted into a fully linked softmax layer for classification purposes [34-35].

2) Multi-Layer Perception (MLP)

The MLP model is a feedforward ANN that is the building block of deep learning and DNN implementations. The input, output, and hidden layers make up the three layers of the MLP. Due to the direct connections between each neuron in each

layer, this network can be called fully connected [36]. After receiving the input data, the input layer normalizes the features and then distributes them across the network. Signals are transmitted from the outputs of this layer to the inputs of the hidden or output layer below it. Many hidden layers, the number of which can be adjusted, handle the signal processing and transmit signals from the input to the output. Hidden layers consist of regular neurons that analyze the data collected from the preceding layer. Their input is the most recent layer's output, and their output is the most recent layer's input. In the output layer, the processed data is used to produce predictions or judgments [37]. The activation function φ, is a nonlinear function that in a single-neuron perceptron model translates the summation function $(xw + b)$ into the output value y:

$$y = \varphi(xw + b) \quad (2)$$

where x is the input vector, w is the weighting vector, b is the bias, and y is the output value.

This study aims to improve model generalization in diverse datasets using a transfer learning method and domain adaptation. The proposed method was designed to handle problems such as class imbalance and domain shift. Deep Transfer Learning (DTL) is the process of employing already learned knowledge in one area to another to map the features or representations learned from a source to a target domain and improve performance [38]. The convolution layers of DenseNet201, pre-trained on the ImageNet dataset, were used to extract high-level features from medical images. Its layers aggregated common patterns that can be leveraged with new activities. This process of modifying the pre-trained DenseNet201 model to accommodate a special medical dataset is called fine-tuning. This involves tweaking the weights of the pre-trained model to fit with the new data and enable it to detect medical abnormalities more accurately. The features extracted from all cells by DenseNet201 are saved in a file to be used during MLP integration and classification. MLP can capture different patterns and nuances in medical data, improving the final accuracy [39].

3) Training of Proposed Model

The model architecture comprises several layers: an image input layer, a DenseNet201 functional layer, and subsequent layers comprising dropout, dense, and flattening layers. In total, 50,306,627 parameters were used. For the whole training process, the Adam optimizer was used with a learning rate of 0.0001 and categorical cross-entropy loss. The activation functions used in the MLP layers consist of Softmax for the final layer and ReLu throughout. A batch size of 32 was employed, and the training process spanned a total of 100 epochs.

E. Performance Evaluation

Accuracy, precision, recall, and F1 score were some of the evaluation criteria used to analyze the performance of the model. The confusion matrix was used to evaluate the classifier's capacity to identify the three classes. The number of accurate predictions is denoted by True Negatives (TN) and True Positives (TP), while the number of wrong predictions is denoted by False Negatives (FN) and False Positives (FP). The performance measures used in this investigation are listed along with brief descriptions and mathematical calculations in [35].

```
Model: "model"
_________________________________________________________________
 Layer (type)                Output Shape              Param #
=================================================================
 image_input (InputLayer)    [(None, 128, 128, 3)]     0

 densenet201 (Functional)    (None, None, None, 1920)  18321984

 flatten (Flatten)           (None, 30720)             0

 MLP_input (Dense)           (None, 1024)              31458304

 dropout (Dropout)           (None, 1024)              0

 MLP_Hidden_layer (Dense)    (None, 512)               524800

 dropout_1 (Dropout)         (None, 512)               0

 dense (Dense)               (None, 3)                 1539

=================================================================
Total params: 50,306,627
Trainable params: 50,077,571
Non-trainable params: 229,056
```

Fig. 5. Model summary.

IV. EXPERIMENTAL RESULTS AND ANALYSIS

This study used a PC running Windows 10 and powered by an Intel Core i5-1035G1 CPU 1.00-1.19 GHz for the experimental testing investigation. The models were implemented using the Python programming language and the Jupyter Notebook. Figure 6 shows the line graph plot of the training and validation loss. From the beginning, the training accuracy was 93% and the validation accuracy was 95%. The accuracy rate varied with increasing the number of epochs and finally reached more than 99% at the 100th epoch for both training and validation sets.

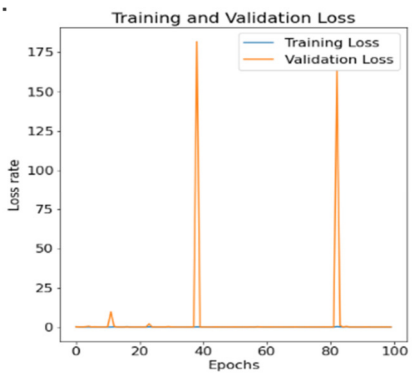

Fig. 6. Training and validation loss graph on the NIH dataset.

The confusion matrix, shown in Figure 7, was also used to evaluate the results of the proposed hybrid DL model. In an instance of COVID detection in a three-class dataset, which included a total of 2880 images as part of the test data, 923 of the images were correctly classified as COVID-19, while two images were incorrectly classified as pneumonia and three of them as normal. Similarly, 946 images were correctly classified as pneumonia, and 977 images were correctly classified as normal cases. Table I represents the final performance results

of the COVID-19 classification. Some additional performance parameters were calculated to evaluate the performance of the proposed model according to specificity, sensitivity, F1 score, recall, and precision. The accuracy values in training, validation, and testing were 99.91%, 99.14%, and 98.82%, respectively, while the loss values were 0.0036, 0.0416, and 0.0590, respectively. In addition to accuracy, sensitivity, specificity, F1 score, recall, and precision were excellent, achieving values close to 99% or higher.

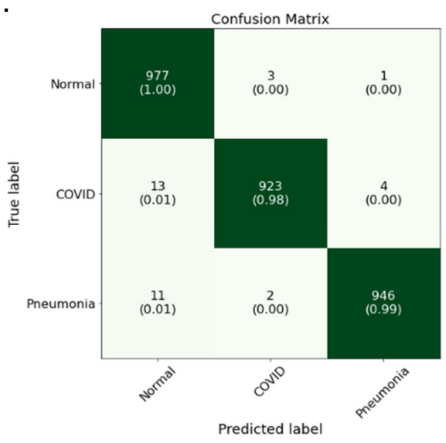

Fig. 7. Confusion matrix.

TABLE II. PERFORMANCE RESULTS OF COVID-19 CLASSIFICATION

Parameters	Performance
Training loss	0.0036
Training accuracy	99.91
Validation loss	0.0416
Validation accuracy	99.14
Testing loss	0.0590
Testing accuracy	98.82
Sensitivity	99.69
Specificity	98.61
F1 score	99
Precision	99

The proposed hybrid of DenseNet201 and MLP exhibited outstanding performance when evaluated on a CXR image dataset. Demonstrating robustness during validation, the model achieved 99.14% accuracy with a loss of 0.0416 after achieving a training accuracy of 99.91% with a training loss of 0.0036 (Figures 8 and 9).

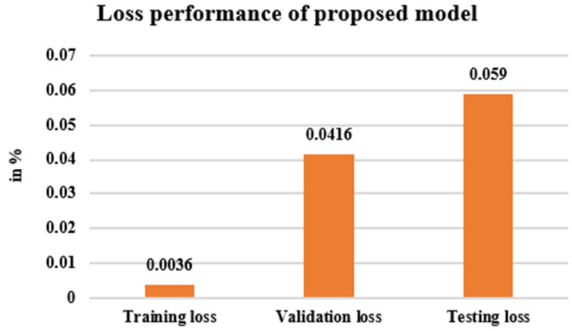

Fig. 8. Bar graph loss of the proposed model.

The test results provide additional evidence of its efficacy, as it achieved 98.82% accuracy with a negligible loss of 0.0590. The model's ability to accurately classify positive and negative instances is underscored by sensitivity and specificity, totaling 99.69% and 98.61%, respectively. Figure 10 shows a visual representation of the model's performance metrics.

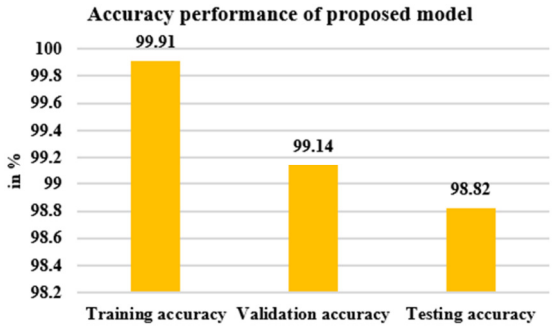

Fig. 9. Accuracy of the proposed model.

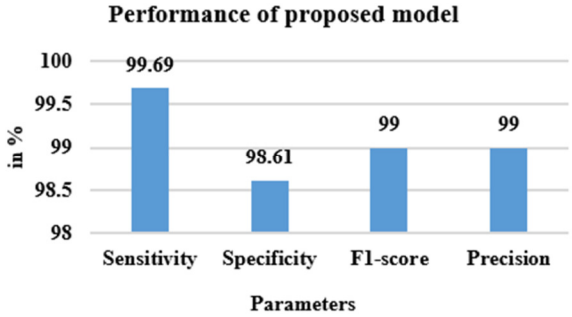

Fig. 10. Performance measures of the proposed model.

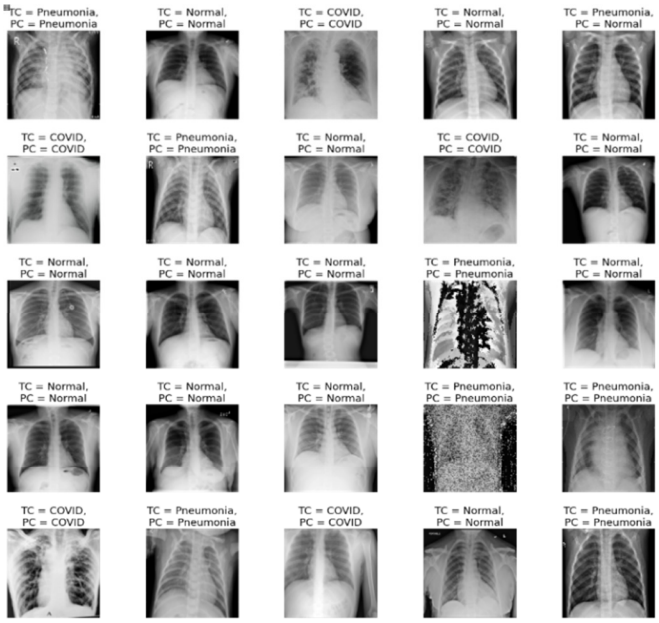

Fig. 11. Prediction results on the CXR image dataset for multiple diseases.

Figure 11 shows some prediction results after testing the proposed model on the CXR image dataset, indicating the

Predicted Class (PC) and True class (TC). The proposed hybrid model outperformed various state-of-the-art COVID-19 CXR detection algorithms with 98.82% accuracy. Its high recall of 99.69% and specificity of 98.61% show its ability to detect positive and negative instances. The model's accuracy and balance are shown by its 99% F1 score and precision metrics.

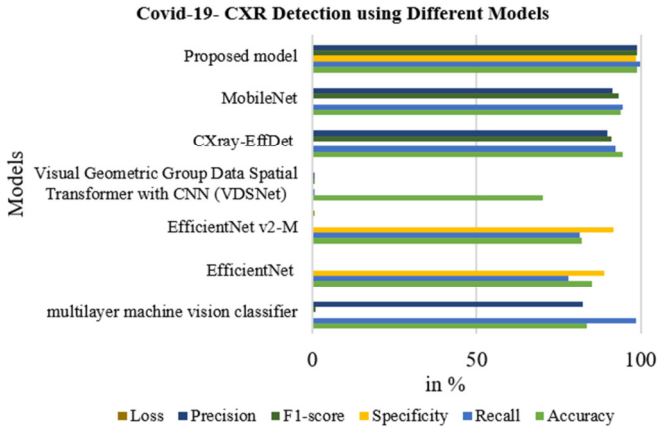

Fig. 12. Comparative performance graph of different models for Covid-19 detection in CXR images.

The proposed method detects COVID-19 in CXR images better than several existing models. Table II and Figure 12 show that the proposed model outperformed other models in accuracy, recall, specificity, F1 score, precision, and loss. This implies that using a hybrid of DenseNet201 and MLP can accurately and reliably detect and classify COVID-19 cases in CXR images. Table II shows the final performance results of the COVID-19 classification in different CXR image datasets, in terms of accuracy and loss.

V. CONCLUSION AND FUTURE WORK

Pre-trained neural networks can be employed for COVID-19 diagnosis. This study used a pre-trained DTL architecture and a conventional DL model to develop an automated instrument to diagnose COVID-19 from CXR images. The proposed method was specifically designed to classify CXR images acquired with portable equipment into three different clinical categories: normal, pneumonia, and COVID-19. The Densenet201 and MLP DL approaches were used. The joint response of these approaches allows for improved differentiation between patients infected with COVID-19, patients with other diseases that manifest characteristics similar to COVID-19, and normal cases. The proposed approach was validated over a dataset specifically retrieved for this research. Despite the poor quality of CXR images, which is inherent in portable equipment, the proposed approach provided excellent global accuracy values of 98.82% and 99%, respectively, allowing for a reliable analysis of portable radiographs to facilitate the clinical decision-making process.

TABLE III. COMPARISON BETWEEN EXISTING TECHNIQUES AND THE PROPOSED MODEL

Reference	Model	Accuracy	Recall	Specificity	F1-score	Precision	Loss
[14]	EfficientNet	85.32	77.97	88.98			
[20]	EfficientNet v2-M	82.15	81.40	91.65			0.6933
[22]	CXray-EffDet	94.53	92.36		91.16	90	
[26]	Visual Geometric Group Data Spatial Transformer with CNN (VDSNet)	70.24	0.63		0.65	0.67	
[31]	multilayer machine vision classifier	83.57	98.68		0.8981	82.42	
[34]	MobileNet	93.75	94.39		93.18	91.36	
Proposed	**Hybrid DenseNet201 and MLP**	**98.82**	**99.69**	**98.61**	**99**	**99**	**0.0590**

Future studies should investigate transfer learning and domain adaptation to enhance the proposed hybrid DenseNet201 and MLP model on varied datasets. Evaluating the model's medical decision-making requires interpretability research. Adding attention mechanisms and clever data augmentation procedures may help the model spot subtle patterns in CXR images. Clinical relevance can be improved by collaborating with domain specialists. To prove its practicality, the model should be tested in real-world healthcare settings and monitored continuously. These efforts seek to make the proposed model a useful and reliable clinical tool for CXR image classification.

DATA AVAILABILITY

The datasets used and analyzed in this study are available in:

- https://www.kaggle.com/prashant268/chest-xray-covid19-pneumonia
- https://www.kaggle.com/tawsifurrahman/covid19-radiography-database
- https://data.mendeley.com/datasets/9xkhgts2s6/1
- https://www.kaggle.com/mdzabirulislam/covid19-chest-xray-image-repository.

REFERENCES

[1] A. K. Sharma, "Novel Coronavirus Disease (COVID-19)," *Resonance*, vol. 25, no. 5, pp. 647–668, May 2020, https://doi.org/10.1007/s12045-020-0981-3.

[2] F. Khatami *et al.*, "A meta-analysis of accuracy and sensitivity of chest CT and RT-PCR in COVID-19 diagnosis," *Scientific Reports*, vol. 10, no. 1, Dec. 2020, Art. no. 22402, https://doi.org/10.1038/s41598-020-80061-2.

[3] L. M. Kucirka, S. A. Lauer, O. Laeyendecker, D. Boon, and J. Lessler, "Variation in False-Negative Rate of Reverse Transcriptase Polymerase Chain Reaction–Based SARS-CoV-2 Tests by Time Since Exposure," *Annals of Internal Medicine*, vol. 173, no. 4, pp. 262–267, Aug. 2020, https://doi.org/10.7326/M20-1495.

[4] C. Qin, D. Yao, Y. Shi, and Z. Song, "Computer-aided detection in chest radiography based on artificial intelligence: a survey," *BioMedical Engineering OnLine*, vol. 17, no. 1, Aug. 2018, Art. no. 113, https://doi.org/10.1186/s12938-018-0544-y.

[5] H. A. Owida, A. Al-Ghraibah, and M. Altayeb, "Classification of Chest X-Ray Images using Wavelet and MFCC Features and Support Vector Machine Classifier," *Engineering, Technology & Applied Science*

Research, vol. 11, no. 4, pp. 7296–7301, Aug. 2021, https://doi.org/10.48084/etasr.4123.

[6] A. N. Zakirov, R. F. Kuleev, A. S. Timoshenko, and A. V. Vladimirov, "Advanced approaches to computer-aided detection of thoracic diseases on chest X-rays," *Applied Mathematical Sciences*, vol. 9, pp. 4361–4369, 2015, https://doi.org/10.12988/ams.2015.54348.

[7] A. G. Yadessa and A. O. Salau, "Low Cost Sensor Based Hand Washing Solution for COVID-19 Prevention," in *2021 International Conference on Innovation and Intelligence for Informatics, Computing, and Technologies (3ICT)*, Zallaq, Bahrain, Sep. 2021, pp. 93–97, https://doi.org/10.1109/3ICT53449.2021.9581821.

[8] K. Carvalho, J. P. Vicente, M. Jakovljevic, and J. P. R. Teixeira, "Analysis and Forecasting Incidence, Intensive Care Unit Admissions, and Projected Mortality Attributable to COVID-19 in Portugal, the UK, Germany, Italy, and France: Predictions for 4 Weeks Ahead," *Bioengineering*, vol. 8, no. 6, Jun. 2021, Art. no. 84, https://doi.org/10.3390/bioengineering8060084.

[9] V. Reshetnikov, O. Mitrokhin, N. Shepetovskaya, E. Belova, and M. Jakovljevic, "Organizational measures aiming to combat COVID-19 in the Russian Federation: the first experience," *Expert Review of Pharmacoeconomics & Outcomes Research*, vol. 20, no. 6, pp. 571–576, Nov. 2020, https://doi.org/10.1080/14737167.2020.1823221.

[10] M. J. Jassim Ghrabat, G. Ma, and C. Cheng, "Towards Efficient for Learning Model Image Retrieval," in *2018 14th International Conference on Semantics, Knowledge and Grids (SKG)*, Guangzhou, China, Sep. 2018, pp. 92–99, https://doi.org/10.1109/SKG.2018.00020.

[11] S. Grima, R. Rupeika-Apoga, M. Kizilkaya, I. Romānova, R. Dalli Gonzi, and M. Jakovljevic, "A Proactive Approach to Identify the Exposure Risk to COVID-19: Validation of the Pandemic Risk Exposure Measurement (PREM) Model Using Real-World Data," *Risk Management and Healthcare Policy*, vol. 14, pp. 4775–4787, Nov. 2021, https://doi.org/10.2147/RMHP.S341500.

[12] M. Chetoui and M. A. Akhloufi, "Explainable Vision Transformers and Radiomics for COVID-19 Detection in Chest X-rays," *Journal of Clinical Medicine*, vol. 11, no. 11, Jan. 2022, Art. no. 3013, https://doi.org/10.3390/jcm11113013.

[13] R. Sahal, S. H. Alsamhi, K. N. Brown, D. O'Shea, and B. Alouffi, "Blockchain-Based Digital Twins Collaboration for Smart Pandemic Alerting: Decentralized COVID-19 Pandemic Alerting Use Case," *Computational Intelligence and Neuroscience*, vol. 2022, no. 1, 2022, Art. no. 7786441, https://doi.org/10.1155/2022/7786441.

[14] A. AlMohimeed, H. Saleh, N. El-Rashidy, R. M. A. Saad, S. El-Sappagh, and S. Mostafa, "Diagnosis of COVID-19 Using Chest X-ray Images and Disease Symptoms Based on Stacking Ensemble Deep Learning," *Diagnostics*, vol. 13, no. 11, Jan. 2023, Art. no. 1968, https://doi.org/10.3390/diagnostics13111968.

[15] S. Lafraxo and M. el Ansari, "CoviNet: Automated COVID-19 Detection from X-rays using Deep Learning Techniques," in *2020 6th IEEE Congress on Information Science and Technology (CiSt)*, Agadir - Essaouira, Morocco, Jun. 2020, pp. 489–494, https://doi.org/10.1109/CiSt49399.2021.9357250.

[16] K. Rezaee, A. Badiei, and S. Meshgini, "A hybrid deep transfer learning based approach for COVID-19 classification in chest X-ray images," in *2020 27th National and 5th International Iranian Conference on Biomedical Engineering (ICBME)*, Tehran, Iran, Nov. 2020, pp. 234–241, https://doi.org/10.1109/ICBME51989.2020.9319426.

[17] T. Anwar and S. Zakir, "Deep learning based diagnosis of COVID-19 using chest CT-scan images," in *2020 IEEE 23rd International Multitopic Conference (INMIC)*, Bahawalpur, Pakistan, Aug. 2020, pp. 1–5, https://doi.org/10.1109/INMIC50486.2020.9318212.

[18] M. J. Ghrabat, G. Ma, P. L. P. Avila, M. J. Jassim, and S. J. Jassim, "Content-based image retrieval of color, shape and texture by using novel multi-SVM classifier," *International Journal of Machine Learning and Computing*, vol. 9, no. 4, pp. 483–489, 2019.

[19] V. Triveni, R. G. Priyanka, K. D. Teja, and Y. Sangeetha, "Programmable Detection of COVID-19 Infection Using Chest X-Ray Images Through Transfer Learning," in *2021 Third International Conference on Inventive Research in Computing Applications (ICIRCA)*, Coimbatore, India, Sep. 2021, pp. 1486–1492, https://doi.org/10.1109/ICIRCA51532.2021.9545050.

[20] E. N. Karajah and M. Awad, "Covid-19 Detection From Chest X-Rays Using Modified VGG 16 Model," in *2021 International Conference on Promising Electronic Technologies (ICPET)*, Deir El-Balah, State of Palestine, Nov. 2021, pp. 46–51, https://doi.org/10.1109/ICPET53277.2021.00015.

[21] A. H. Al Majid *et al.*, "Comparison of Models Architecture on Chest X-Ray Image Classification With Transfer Learning Algorithms," in *2021 5th International Conference on Informatics and Computational Sciences (ICICoS)*, Semarang, Indonesia, Nov. 2021, pp. 171–175, https://doi.org/10.1109/ICICoS53627.2021.9651771.

[22] S. Kim, B. Rim, S. Choi, A. Lee, S. Min, and M. Hong, "Deep Learning in Multi-Class Lung Diseases' Classification on Chest X-ray Images," *Diagnostics*, vol. 12, no. 4, 2022, https://doi.org/10.3390/diagnostics12040915.

[23] M. Kaur, V. Kumar, V. Yadav, D. Singh, N. Kumar, and N. N. Das, "Metaheuristic-based Deep COVID-19 Screening Model from Chest X-Ray Images," *Journal of Healthcare Engineering*, vol. 2021, no. 1, 2021, Art. no. 8829829, https://doi.org/10.1155/2021/8829829.

[24] M. Gupta, N. Kumar, N. Gupta, and A. Zaguia, "Fusion of multi-modality biomedical images using deep neural networks," *Soft Computing*, vol. 26, no. 16, pp. 8025–8036, Aug. 2022, https://doi.org/10.1007/s00500-022-07047-2.

[25] Z. A. Oraibi and S. Albasri, "Predicting COVID-19 from Chest X-ray Images using a New Deep Learning Architecture," in *2022 IEEE Applied Imagery Pattern Recognition Workshop (AIPR)*, Oct. 2022, https://doi.org/10.1109/AIPR57179.2022.10092231.

[26] M. Nawaz, T. Nazir, J. Baili, M. A. Khan, Y. J. Kim, and J.-H. Cha, "CXray-EffDet: Chest Disease Detection and Classification from X-ray Images Using the EfficientDet Model," *Diagnostics*, vol. 13, no. 2, 2023, https://doi.org/10.3390/diagnostics13020248.

[27] N. Kumar, A. Hashmi, M. Gupta, and A. Kundu, "Automatic Diagnosis of Covid-19 Related Pneumonia from CXR and CT-Scan Images," *Engineering, Technology & Applied Science Research*, vol. 12, no. 1, pp. 7993–7997, Feb. 2022, https://doi.org/10.48084/etasr.4613.

[28] I. Abdelli, F. Hassani, S. Bekkel Brikci, and S. Ghalem, "In silico study the inhibition of angiotensin converting enzyme 2 receptor of COVID-19 by Ammoides verticillata components harvested from Western Algeria," *Journal of Biomolecular Structure and Dynamics*, vol. 39, no. 9, pp. 3263–3276, Jun. 2021, https://doi.org/10.1080/07391102.2020.1763199.

[29] S. Latif *et al.*, "Leveraging Data Science to Combat COVID-19: A Comprehensive Review," *IEEE Transactions on Artificial Intelligence*, vol. 1, no. 1, pp. 85–103, Dec. 2020, https://doi.org/10.1109/TAI.2020.3020521.

[30] T. K. K. Ho, J. Gwak, O. Prakash, J. I. Song, and C. M. Park, "Utilizing Pretrained Deep Learning Models for Automated Pulmonary Tuberculosis Detection Using Chest Radiography," in *Intelligent Information and Database Systems*, 2019, pp. 395–403, https://doi.org/10.1007/978-3-030-14802-7_34.

[31] Md. M. Islam, T. Hannan, L. Sarker, and Z. Ahmed, "COVID-DenseNet: A Deep Learning Architecture to Detect COVID-19 from\ Chest Radiology Images," in *Proceedings of International Conference on Data Science and Applications*, Kolkata, India, 2023, pp. 397–415, https://doi.org/10.1007/978-981-19-6634-7_28.

[32] M. Jalil Jassim Ghrabat *et al.*, "Fully automated model on breast cancer classification using deep learning classifiers," *Indonesian Journal of Electrical Engineering and Computer Science*, vol. 28, no. 1, pp. 183-191, Oct. 2022, https://doi.org/10.11591/ijeecs.v28.i1.pp183-191.

[33] D. Jain and V. Singh, "A two-phase hybrid approach using feature selection and Adaptive SVM for chronic disease classification," *International Journal of Computers and Applications*, vol. 43, no. 6, pp. 524–536, Jul. 2021, https://doi.org/10.1080/1206212X.2019.1577534.

[34] N. V. Chawla, K. W. Bowyer, L. O. Hall, and W. P. Kegelmeyer, "SMOTE: Synthetic Minority Over-sampling Technique," *Journal of Artificial Intelligence Research*, vol. 16, pp. 321–357, Jun. 2002, https://doi.org/10.1613/jair.953.

[35] K. C. Ke and M. S. Huang, "Quality Prediction for Injection Molding by Using a Multilayer Perceptron Neural Network," *Polymers*, vol. 12, no. 8, 2020, https://doi.org/10.3390/polym12081812.

[36] S. H. Wang and Y. D. Zhang, "DenseNet-201-Based Deep Neural Network with Composite Learning Factor and Precomputation for Multiple Sclerosis Classification," *ACM Transactions on Multimedia Computing, Communications, and Applications*, vol. 16, no. 2s, Mar. 2020, https://doi.org/10.1145/3341095.

[37] M. S. Choudhari, "Breast Cancer Detection using Deep Learning Techniques," *International Journal for Research in Applied Science and Engineering Technology*, vol. 9, no. VI, pp. 3959–3963, Jun. 2021, https://doi.org/10.22214/ijraset.2021.35757.

[38] G. Nguyen *et al.*, "Machine Learning and Deep Learning Frameworks and Libraries for Large-Scale Data Mining: A Survey," *Artificial Intelligence Review*, vol. 52, no. 1, pp. 77–124, Jun. 2019, https://doi.org/10.1007/s10462-018-09679-z.

[39] Q. Tang, N. Sang, and H. Liu, "Contrast-dependent surround suppression models for contour detection," *Pattern Recognition*, vol. 60, pp. 51–61, Dec. 2016, https://doi.org/10.1016/j.patcog.2016.05.009.